Biochimica et Biophysica Acta 1837 (2014) 1595–1601

Contents lists available at ScienceDirect

Biochimica et Biophysica Acta

journal homepage: www.elsevier.com/locate/bbabio

A simple method to engineer a protein-derived redox cofactor for catalysis

Sooim Shin [a,1], Moonsung Choi [b,1], Heather R. Williamson [a], Victor L. Davidson [a,*]

[a] Burnett School of Biomedical Sciences, College of Medicine, University of Central Florida, Orlando, FL 32827, USA
[b] Seoul National University of Science and Technology, College of Energy and Biotechnology, Department of Optometry, Seoul, 139-743, Republic of Korea

ARTICLE INFO

Article history:
Received 3 February 2014
Received in revised form 14 May 2014
Accepted 16 May 2014
Available online 22 May 2014

Keywords:
Protein Engineering
Enzyme
Biotechnology
Bioenergetics
Histidine tag

ABSTRACT

The 6×-Histidine tag which is commonly used for purification of recombinant proteins was converted to a catalytic redox-active center by incorporation of Co^{2+}. Two examples of the biological activity of this engineered protein-derived cofactor are presented. After inactivation of the natural diheme cofactor of MauG, it was shown that the Co^{2+}-loaded 6×His-tag could substitute for the hemes in the H_2O_2-driven catalysis of tryptophan tryptophylquinone biosynthesis. To further demonstrate that the Co^{2+}-loaded 6×His-tag could mediate long range electron transfer, it was shown that addition of H_2O_2 to the Co^{2+}-loaded 6×His-tagged Cu^{1+} amicyanin oxidizes the copper site which is 20 Å away. These results provide proof of principle for this simple method by which to introduce a catalytic redox-active site into proteins for potential applications in research and biotechnology.

1. Introduction

This paper describes a simple procedure for the introduction of a high-potential oxidizing species into a specific location on a protein using standard molecular biology techniques. This is done by adding cobalt to a polyhistidine tag that is commonly used for protein purification. We show that this engineered cofactor is competent in both oxidative catalysis and electron transfer. Two examples that demonstrate the biological activity of this engineered protein-derived cofactor are presented. It was shown that the Co^{2+}-loaded 6×His-tag could substitute for the natural diheme cofactor of MauG in H_2O_2-driven tryptophan tryptophylquinone (TTQ) biosynthesis after inactivation of the native hemes. It was also shown that the Co^{2+}-loaded 6×His-tag could mediate long range electron transfer when attached to the cupredoxin amicyanin.

MauG is a *c*-type diheme enzyme [1] which catalyzes posttranslational modifications of methylamine dehydrogenase (MADH) [2] that complete the formation of the protein-derived TTQ [3] cofactor (Fig. 1). This catalytic reaction requires a 6-electron oxidation of two specific tryptophan residues of the protein substrate [4]. These oxidation reactions proceed via a bis-Fe^{IV} redox form of the two hemes [5] of MauG in which one heme is Fe^{IV}=O with a His axial ligand and the other is Fe^{IV} with axial heme ligands provided by His and Tyr side chains [6]. Catalysis requires long range electron transfer from the preTTQ substrate to the Fe^{IV} hemes of MauG (Fig. 1) which was shown to occur via a hole hopping mechanism [7,8] of electron transfer in which Trp residues of MauG are reversibly oxidized [9,10]. A tightly bound Ca^{2+} is present in MauG which is positioned in the vicinity of the two hemes and which is connected to each heme via H-bonding networks that include bound waters [6]. Removal of this Ca^{2+} by chelators yields a Ca^{2+}-depleted MauG which has no TTQ biosynthesis activity [11]. This is due to changes in the diheme site which prevent formation of the bis-Fe^{IV} state [12]. Whereas addition of H_2O_2 to native MauG generates the bis-Fe^{IV} state, the hemes of Ca^{2+}-depleted MauG are not reactive towards H_2O_2. The recombinant MauG used in these previous studies possesses a 6×His-tag at the C-terminal end of the protein which was added to facilitate purification. It is located ~35 Å from the preTTQ site of preMADH and 27 Å from Trp199 which mediates the hole hopping that is required for catalysis [9] (Fig. 1). This study investigated the possibility that Co^{2+} could be incorporated into the 6×His-tag and converted by H_2O_2 to a potent oxidant that could substitute for the inactive hemes in Ca^{2+}-depleted MauG in catalyzing TTQ-biosynthesis. The results describe the functionality of the Co^{2+}-loaded 6×His-tag in the catalytic reaction of MauG-dependent TTQ biosynthesis.

For additional proof of principle of this approach, the ability of a Co^{2+}-loaded 6×His-tag to participate in another long range electron transfer reaction was also demonstrated. This study used a type I copper

Abbreviations: 6×His-tag, 6x-Histidine; TTQ, tryptophan tryptophylquinone; MADH, methylamine dehydrogenase; preMADH, the biosynthetic precursor protein of MADH with incompletely synthesized TTQ; ET, electron transfer; *bis*-Fe^{IV} MauG, redox state of MauG with one heme as Fe^{IV}=O and the other as Fe^{IV}

* Corresponding author at: Burnett School of Biomedical Sciences, College of Medicine, University of Central Florida, 6900 Lake Nona Blvd., Orlando, FL 32827, USA. Tel.: +1 407 266 7111; fax: +1 407 266 7002.
E-mail address: victor.davidson@ucf.edu (V.L. Davidson).

[1] These authors contributed equally to this work.

http://dx.doi.org/10.1016/j.bbabio.2014.05.354
0005-2728/

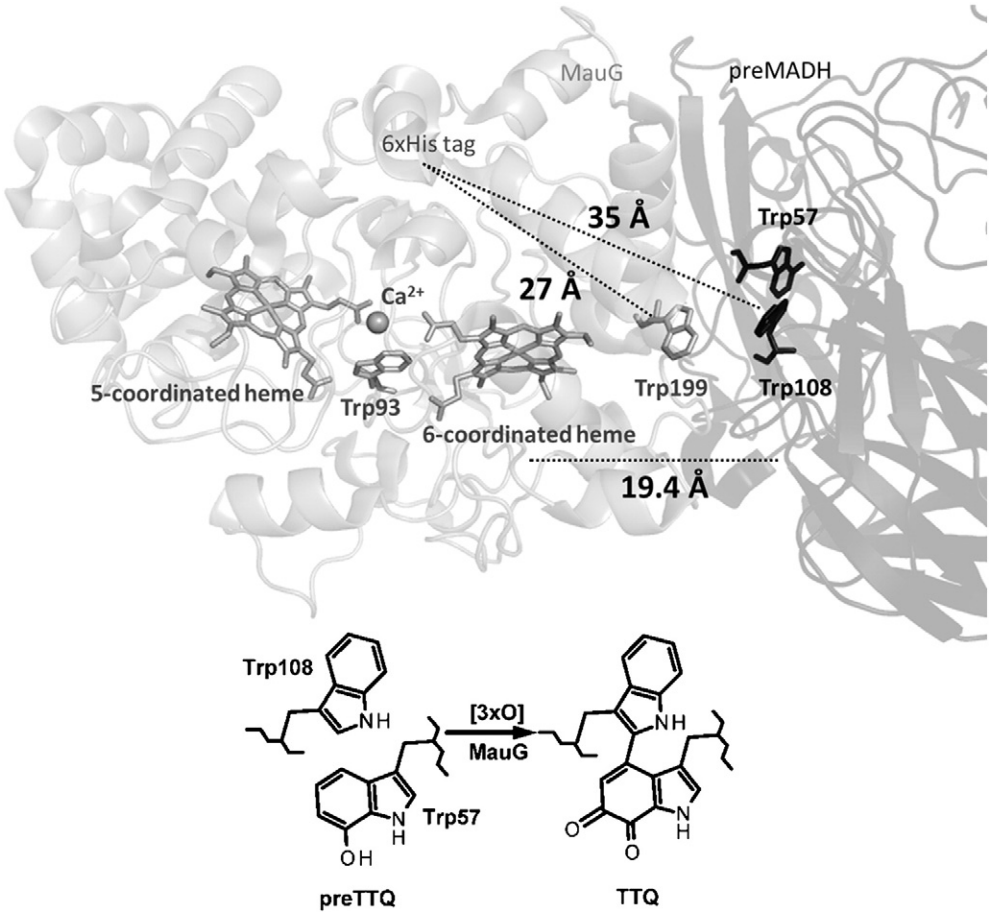

Fig. 1. The MauG-preMADH complex and the reaction that it catalyzes. The structure of the MauG-preMADH complex from *P. denitrificans* (PDB ID: 3L4M) is displayed with the hemes, Ca^{2+} and residues of interest indicated. The distances from the 6×His-tag site at the C-terminus of MauG to the preTTQ site, and from the nearest heme of MauG to the preTTQ site are indicated. The reaction catalyzed by MauG is shown below the structure. [O] represents oxidizing equivalents which may be provided by H_2O_2.

protein, amicyanin from *Paracoccus denitrificans* [13,14] with a 6×His-tag added to the N-terminus of the protein. Type 1 copper sites are found in a wide range of redox proteins in bacteria, plants and animals, and function as electron transfer mediators [15,16]. In the type 1 site a single copper is coordinated by three equatorial ligands that are provided by a Cys and two His residues, and by a fourth weak axial ligand, usually provided by a Met and they are characterized by an intense blue color and absorption centered near 600 nm that result from a $S(Cys)\pi \rightarrow Cu(II)d_{x2-y2}$ ligand-to-metal charge transfer transition [17]. It was shown that the 6×His-tag-bound Co^{2+} can be oxidized by H_2O_2 and subsequently oxidize the Cu^{1+} of reduced amicyanin via intraprotein electron transfer over a distance of over 20 Å. This system was also used to characterize some of the properties of the Co^{2+}-loaded 6×His-tag site. These studies illustrate the utility of a relatively simple and inexpensive method for the introduction of a potent oxidizing species into a specific site on a protein for potential use as a catalyst or electron transfer mediator.

2. Materials and methods

2.1. Protein expression and preparation

Recombinant MauG is produced in a homologous expression system using *P. denitrificans* [1]. The *mauG* gene was fused with the promoter region of the *cycA* (cytochrome *c*-550) gene [18] of *P. denitrificans* that was cloned into the pBluescript II KS(+) vector. A 6×His-tag was inserted by site-directed mutagenesis at the C-terminal of *mauG*. The cycA promoter-*mauG*-6×His segment was excised and ligated into pRK415-1, a broad-host-range vector. This plasmid was introduced into *P. denitrificans* by conjugation with the mobilizing *Escherichia coli* strain S17-1. As the N-terminal signal sequence of *mauG* was retained, the 6×His tagged MauG protein was isolated directly from the periplasmic fraction using Ni-NTA Superflow resin. It was eluted from the Ni-NTA resin in 70 mM imidazole. Ca^{2+}-depleted MauG was prepared by incubation of native MauG with 0.01 M EDTA disodium salt [11]. Methods for the expression and purification of recombinant preMADH, the substrate for MauG, from a *Rhodobacter sphaeroides* expression system were as described previously [19].

Amicyanin is encoded by the *mauC* gene of *P. denitrificans* [20]. The *mauC* gene was cloned into a pUC19 vector and a 6×His-tag was inserted by site-directed mutagenesis between the codon of the N-terminal amino acid and the native signal sequence of the gene which directs expression of the mature protein into the periplasmic space. This plasmid was introduced into *E. coli* strain BL-21(DE3) to express the 6×His-tagged amicyanin. The recombinant protein was purified from the periplasmic fraction of the harvested cells which was prepared by treatment with lysozyme followed by a mild osmotic shock [21]. This fraction was subjected to chromatography using a Ni-NTA Superflow resin and the 6×His-tagged amicyanin was eluted from the resin with 70 mM imidazole. MADH [22] and cytochrome *c*-551i [23] were purified from *P. denitrificans* as described previously.

2.2. Mechanistic studies

The steady-state spectrophotometric assay of MauG-dependent TTQ biosynthesis using preMADH as the substrate was performed using H_2O_2 as the source of oxidizing equivalents as was previously described [24]. The reaction was performed in 0.05 M Tris–HCl buffer, pH 7.5.

The redox state of the copper of amicyanin was monitored by absorbance spectrophotometry. The Cu^{2+} protein exhibits an $\varepsilon_{595} = 4600$ M^{-1} cm^{-1} while the Cu^{1+} protein is colorless [13]. To generate the reduced (Cu^{1+}) protein, stoichiometric ascorbate was added to oxidized amicyanin. The experiments were performed in 0.05 M Tris–HCl buffer, pH 7.5.

High-resolution size-exclusion chromatography of protein mixtures was performed using a HiPrep 16/60 Sephacryl S-300 HR column on a DuoFlow FPLC system (BioRad). The column was equilibrated and eluted at 0.5 mL/min with 10 mM Tris–HCl, pH 8.0, containing 150 mM NaCl. The column was calibrated using the following molecular mass markers: MauG (43 kDa), cytochrome *c*-553 (30 kDa), and native amicyanin (12.5 kDa).

3. Results

3.1. Co^{2+}-loaded 6×His-tag mediated TTQ biosynthesis by Ca^{2+}-depleted MauG

Ca^{2+}-depleted MauG was incubated with excess $CoCl_2$ to load the 6×His-tag with Co^{2+}. Excess unbound Co^{2+} was removed by buffer exchange. A steady-state assay for the overall reaction of MauG-dependent TTQ biosynthesis from preMADH had been developed in which TTQ formation was monitored by the increase in absorbance centered at 440 nm which is characteristic of TTQ in MADH [24]. Addition of H_2O_2 to the preMADH substrate alone resulted in no TTQ biosynthesis. The formation of TTQ after addition of H_2O_2 in the assay with native MauG is shown in Fig. 2A. For 6×His-tagged Ca^{2+}-depleted MauG without added Co^{2+} the addition of H_2O_2 yields no detectable activity (Fig. 2B). For the Co^{2+}-loaded 6×His-tagged Ca^{2+}-depleted MauG addition of H_2O_2 did result in TTQ biosynthesis (Fig. 2C). Removal of Ca^{2+} from MauG causes changes in the visible absorbance spectrum which are reversible, as re-addition of Ca^{2+} restores the native spectrum [11]. The Co^{2+}-loaded 6×His-tagged Ca^{2+}-depleted MauG was generated by incubation with 0.1 mM $CoCl_2$. The incubation with Co^{2+} did not reverse the changes in the absorbance spectrum indicating that it did not simply bind to the native Ca^{2+}-binding site. To more thoroughly address the possibility that Co^{2+} will simply occupy the Ca^{2+} cite in MauG, the addition of other divalent metal cations was also tested. The 6×His-tagged Ca^{2+}-depleted MauG was incubated with either 1 mM $NiSO_4$, 10 mM $ZnCl_2$, 5 mM $MnSO_4$, 0.1 mM $FeSO_4$, or 0.5 mM $CuSO_4$. None of these divalent metal cations restored the native absorbance spectrum or resulted in a protein that was active in the reaction of TTQ biosynthesis from preMADH. Thus the native Ca^{2+}-binding site is highly specific for Ca^{2+} and is not simply being replaced by Co^{2+}.

The reaction rate of the Co^{2+}-loaded 6×His-tagged Ca^{2+}-depleted MauG was slower than that of native MauG exhibiting a k_{cat} of 0.02 s^{-1} compared to 0.16 s^{-1} for native MauG (Fig. 3A). However, in each case the reaction goes to completion. To confirm that the product of the reaction catalyzed by Co^{2+}-loaded 6×His-tagged Ca^{2+}-depleted MauG was the functional TTQ on MADH, the methylamine substrate for MADH was added, and this caused bleaching of the 440 nm absorbance concomitant with the appearance of a peak at 330 nm (Fig. 3B) which is characteristic of substrate-reduced MADH [25].

The reaction catalyzed by native MauG occurs by remote catalysis during which long range electron transfer to the hemes of bis-Fe^{IV} MauG is coupled to radical-mediated reactions which generate the TTQ cofactor [26]. Trp199 of MauG, which resides on the surface of MauG midway between the preTTQ site and the nearest heme (Fig. 1), has been shown to mediate a multistep hopping mechanism of long-range electron transfer that is required for TTQ biosynthesis [9,10]. To determine whether the biosynthetic reaction catalyzed by the Co^{2+}-loaded 6×His-tag on Ca^{2+}-depleted MauG occurs via a similar hopping mechanism, this experiment was repeated using W199F MauG. It was previously shown that W199F MauG reacts with H_2O_2 to form the bis-Fe^{IV} state but is not able to synthesize TTQ from preMADH because hopping cannot occur via the Phe [9]. A Co^{2+}-loaded 6×His-tagged W199F MauG was prepared and assayed and it did not exhibit any TTQ biosynthesis activity (Fig. 2D). This demonstrated that Trp199 also plays a crucial functional role in catalysis by the Co^{2+}-loaded 6×His-tag on Ca^{2+}-depleted MauG and that the Co^{2+}-loaded 6×His-tag has effectively

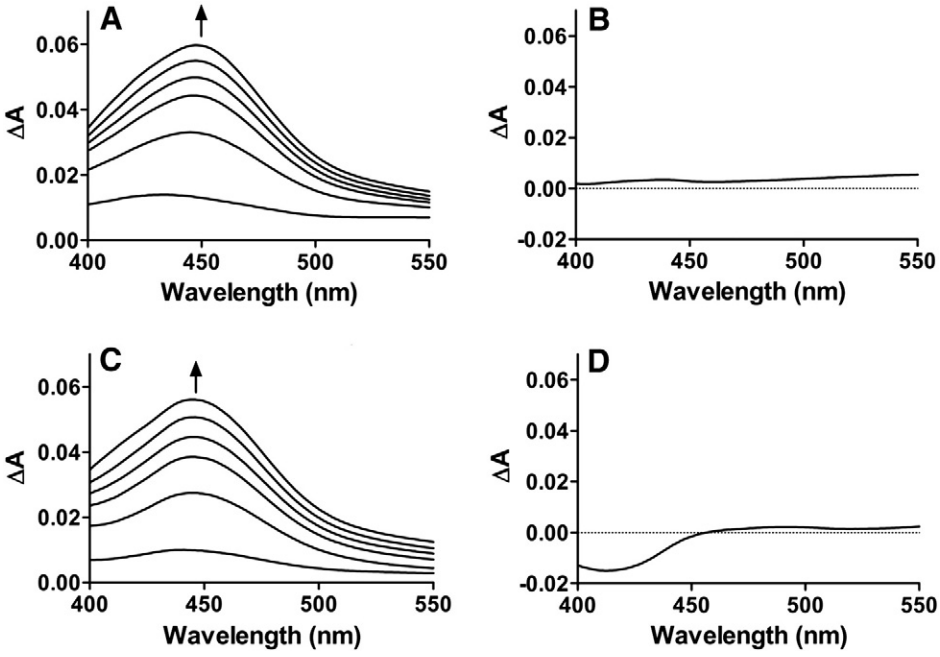

Fig. 2. Spectrophotometric assay of TTQ biosynthesis. Each reaction mixture contained 5 μM preMADH in 10 mM potassium phosphate at pH 7.5 and each reaction was initiated by addition of 100 μM H_2O_2. The forms of MauG used in each assay were (A) native MauG, (B) 6×His-tagged Ca^{2+}-depleted MauG, (C) Co^{2+}-loaded 6×His-tagged Ca^{2+}-depleted MauG and (D) Co^{2+}-loaded 6×His-tagged W199F MauG. In each case the initial spectrum of the mixture before addition of H_2O_2 was subtracted from the recorded spectrum to clearly show the spectral changes that occurred during the reaction. The spectra B and D were recorded 10 min after addition of H_2O_2. The spectra in A were recorded 1, 2, 3, 4, 6 and 10 min after addition of H_2O_2. The spectra in C were recorded 1, 3, 4, 5, 7 and 10 min after addition of H_2O_2.

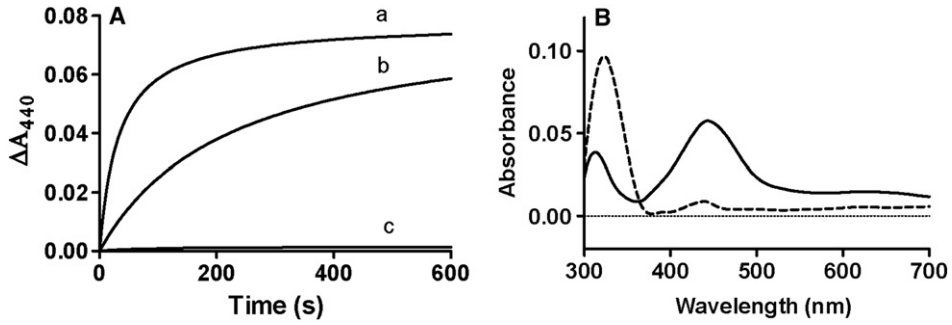

Fig. 3. Time course and confirmation of TTQ biosynthesis by Co^{2+}-loaded 6×His-tagged Ca^{2+}-depleted MauG. A) Time courses of the assays of TTQ biosynthesis for the experiments shown in Fig. 2 for (a) native MauG, (b) Co^{2+}-loaded 6×His-tagged Ca^{2+}-depleted MauG and (c) Ca^{2+}-depleted MauG. B) Spectrum of the final product of the reaction in (b) before (solid line) and after addition of 1 mM methylamine (dashed line).

replaced the inactive hemes as the catalytic cofactor. Furthermore, addition of H_2O_2 to Co^{2+}-loaded 6×His-tagged Ca^{2+}-depleted MauG in the absence of the preMADH substrate did not cause spectroscopic changes associated with the formation of the bis-Fe^{IV} redox state of the hemes. This indicates that the Co^{2+} is not simply mediating the oxidation of the heme irons by H_2O_2. It is indeed substituting for the hemes as a redox cofactor that catalyzes oxidation of the preMADH substrate by a mechanism of remote catalysis. Unfortunately the 6×His-tag is not visible in the X-ray crystal structure of MauG so the exact distance for this reaction is not known but can be estimated from the position of the C-terminus of the protein. The slower rate for the reaction of Co^{2+}-loaded 6×His-tagged Ca^{2+}-depleted MauG with preMADH, compared to native MauG, is likely due to the greater distance between the His-tag site and Trp199 than that from the nearest heme, requiring an increase in the distance for the required through-protein electron transfer (Fig. 1).

3.2. Co^{2+}-loaded 6×His-tag mediated electron transfer through amicyanin

The properties of the 6×His-tagged amicyanin were identical to those of native amicyanin. The absorbance spectrum and oxidation–reduction midpoint potential values were the same. The electron transfer activities of amicyanin with its electron donor, MADH [22], and with its electron acceptor, cytochrome *c*-551i [23], were not affected by the presence of the 6×His-tag. This tag was added to the N-terminal end of the protein which is located 22.5 Å from the copper in the type 1 site of amicyanin (Fig. 4). Again, the His-tag was not apparent in the crystal structure, presumably due to mobility. The 6×His-tagged amicyanin was incubated with excess $CoCl_2$ to load the 6×His-tag with Co^{2+}. This incubation caused an increase in absorbance in the region from 300 to 400 nm (Fig. 5A). The absorbance at 595 nm which is due to the Cu^{2+} in the type 1 site is not affected. It was difficult to observe this cobalt-dependent feature in the absorbance spectrum at 300–400 nm of the Co^{2+}-loaded 6×His-tagged MauG (discussed earlier) because of the significant absorbance of the two hemes in this region of the spectrum. This spectral change provides a means to assess the stoichiometry of Co^{2+} binding to 6×His-tagged amicyanin. Titration of this spectral change with $CoCl_2$ indicates that it is maximal after addition of approximately two Co^{2+} per amicyanin (80 μM $CoCl_2$ to 40 μM 6×His-tagged amicyanin in Fig. 5B and C). Addition of $CoCl_2$ to the native untagged amicyanin resulted in no change in visible absorbance. Thus, this spectral change cannot be attributed to non-specific binding of Co^{2+} elsewhere on the protein and it appears that two Co^{2+} ions are specifically binding to the His-tag.

As was previously reported for native amicyanin [27], the Cu^{1+} state of 6×His-tagged amicyanin that is formed by reduction by ascorbate was very stable against reoxidation under aerobic conditions. The 6×His-tagged Cu^{2+} amicyanin was incubated with excess $CoCl_2$ to load the 6×His-tag with Co^{2+}. Then unbound Co^{2+} was removed by buffer exchange. Amicyanin exhibits a broad absorbance centered at 595 nm in the Cu^{2+} state. The addition of Co^{2+} to the 6×His-tagged amicyanin had no effect on this absorbance feature. Reduction of amicyanin by ascorbate to the Cu^{1+} state causes complete bleaching of the 595 nm absorbance feature. Addition of H_2O_2 to the reduced Co^{2+}-loaded 6×His-tagged amicyanin caused the reappearance of the absorbance around 595 nm, indicating that Cu^{1+} had been oxidized to Cu^{2+} (Fig. 6A, B). A series of control experiments were performed to insure that the oxidation of the copper site was not due to direct reaction with H_2O_2, external or non-specifically bound cobalt, or interprotein electron transfer between protein molecules. Addition of H_2O_2 to the reduced 6×His-tagged amicyanin which had not been incubated with Co^{2+} had no effect, confirming that the bound Co^{2+} is required for this reaction. Addition of H_2O_2 to the reduced untagged native amicyanin had no effect. This experiment was also repeated using native untagged amicyanin in the presence of 10 mM $CoCl_2$ and again addition of H_2O_2 to the reduced untagged native amicyanin had no effect under these conditions. This ruled out the possibility that the observed oxidation of Cu^{1+} was mediated by residual Co^{2+} that was present in the solution, or bound non-specifically to the surface of amicyanin, rather than specifically to the 6×His-tag-coordinated Co^{2+}. To confirm that the reaction is intraprotein electron transfer, the dependence of the

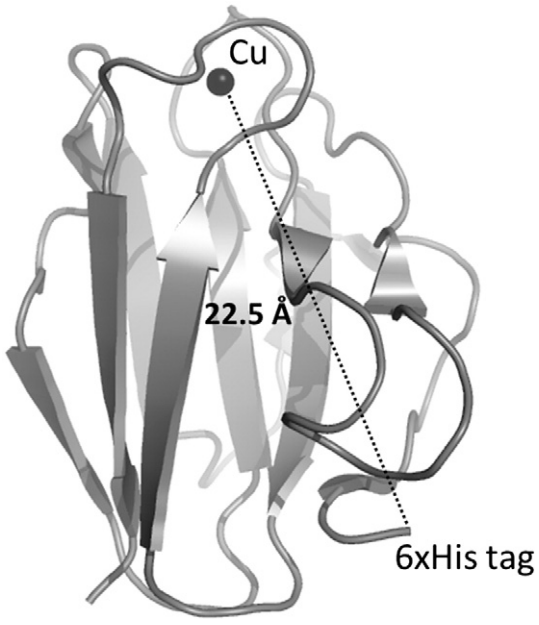

Fig. 4. Positions of the 6×His-tag and copper in amicyanin. The structure of amicyanin from *P. denitrificans* (PDB ID: 2OV0) is displayed with β-sheets and β-turns indicated. The structure contains no α-helices. The copper is displayed as a sphere and the direct distance from the copper to the 6×His-tag site at the N-terminus of the protein is indicated by a dotted line.

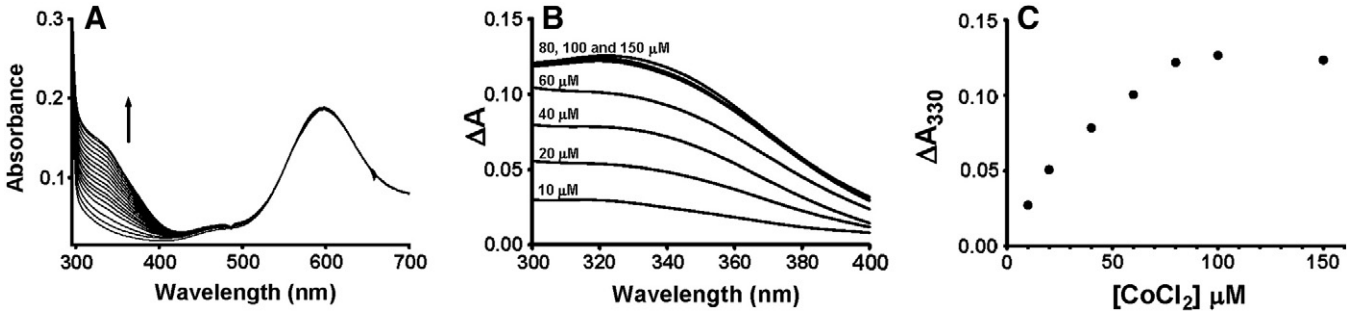

Fig. 5. Spectral changes associated with cobalt binding to 6×His-tagged amicyanin. A) 100 μM $CoCl_2$ was incubated with 40 μM 6×His-tagged amicyanin in 50 mM Tris–HCl buffer at pH 7.5. The spectra were recorded every 2 min. B) $CoCl_2$ was added to 40 μM 6×His-tagged amicyanin in increasing concentrations and the magnitude of the cobalt-induced spectral changes was recorded after reaching the maximum. In each case the initial spectrum of the mixture before addition of $CoCl_2$ was subtracted from the final recorded spectrum to show direct absorbance changes. The final concentrations of $CoCl_2$ are indicated above each trace. C) Absorbance changes at 330 nm are plotted against the $CoCl_2$ concentrations.

observed rate of the reaction on the concentration of Co^{2+}-loaded 6×His-tagged amicyanin was determined. The rate of the reaction was independent of the concentration Co^{2+}-loaded 6×His-tagged amicyanin which is consistent with an intraprotein electron transfer. If electron transfer was instead between the activated Co^{3+} of one protein molecule and the Cu^{1+} of another protein molecule, then second-order kinetics and a linear dependence of rate on protein concentration would have been observed. It is possible that the reactive protein could be a complex in which the bound Co^{2+} ions are present in a dimeric amicyanin complex in which metal ligands are provided by two protein molecules. This would also yield kinetics that was independent of the concentration Co^{2+}-loaded 6×His-tagged amicyanin. To rule out this possibility, the behavior of native and Co^{2+}-loaded 6×His-tagged amicyanin was examined using size-exclusion chromatography. The results indicate that the Co^{2+}-loaded 6×His-tagged amicyanin elutes in a position identical to that of native untagged amicyanin with a mass corresponding to that of a monomer (Fig. 7).

In order to gain some insight into the mechanism by which H_2O_2 interacts with the Co^{2+}-loaded 6×His-tag the rate of reaction of the Co^{2+}-loaded 6×His-tag mediated oxidation of Cu^{1+} by H_2O_2 was examined as a function of H_2O_2 concentration (Fig. 8). A hyperbolic dependence of rate on $[H_2O_2]$ is observed and is consistent with a two-step mechanism in which an initial rapid reversible binding interaction is followed by a rate-limiting reaction step. In this case the initial step is proposed to be the formation of a peroxo-cobalt complex and the subsequent rate-limiting reaction step is the long range electron transfer from Cu^{1+} to Co^{3+}. Oxidation of Co^{2+} to Co^{3+} within the peroxo-cobalt complex is much faster than the subsequent long range electron transfer and so it is not kinetically distinguishable. A fit of these data to Eq. (1) yields a limiting first-order rate constant (k_{ET}) of 7.0×10^{-3} s^{-1} and a $K_d = 234$ μM for H_2O_2. No reverse electron transfer reaction (k_{-ET}) was detected.

$$k_{obs} = k_{ET}[H_2O_2]/([H_2O_2] + K_d) + k_{-ET} \quad (1)$$

In order to assess whether or not the observed rate of the reaction was reasonable for a true electron transfer reaction, the maximum possible electron transfer rate from Cu^{1+} to Co^{3+} under activationless conditions (i.e., $-\Delta G^{o} =$ reorganization energy) [28] was calculated using the HARLEM program [29] and the direct distance approach of Dutton and co-workers [30]. Since the Co^{2+}-loaded 6×His was not visible in the crystal structure its exact position is unknown. As such the calculation was based on the positions of the copper and the C of Asp1, the N-terminal residue. This yielded a predicted maximal rate of 3.5×10^{-2} s^{-1}. This is only about five-fold greater than the experimentally determined first-order rate constant of 7.0×10^{-3} s^{-1} which was determined under optimal conditions. While the calculated rate is only an approximation, it does indicate that the experimentally-determined rate is reasonable for this long range electron transfer reaction. It also suggests that that despite the seemingly slow rate, the Co^{2+}-loaded 6×His-tag functions quite efficiently for electron transfer over a distance of over 20 Å.

4. Discussion

There is a growing interest in developing protein engineering strategies to create or modify existing proteins that possess desired functions with practical applications in biotechnology and research. Many such applications require redox enzymes that can selectively oxidize or reduce substrates. Redox proteins typically possess redox-active

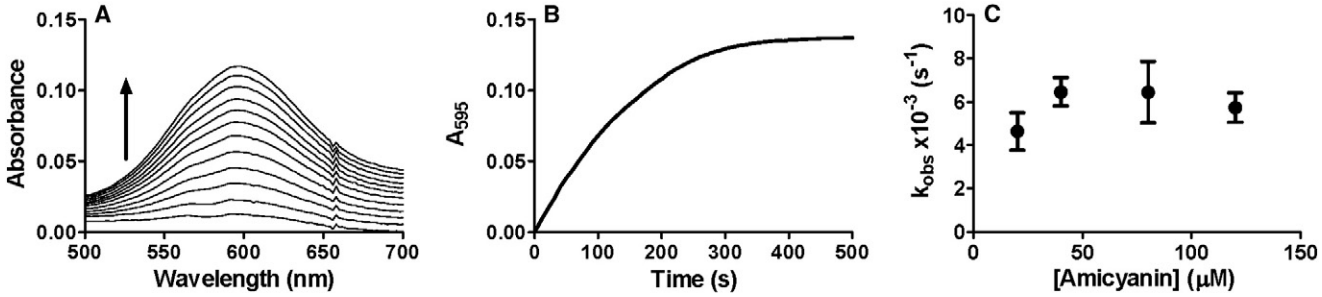

Fig. 6. The reactivity of the Co^{2+}-loaded 6×His-tagged amicyanin. A) Changes in the absorption spectrum of the reduced (Cu^{1+}) protein after addition of 1 mM H_2O_2. The spectra were recorded every 10 s and the arrow shows the direction of the changes. B) Time course of the increase in absorbance at 595 nm from the data shown in (A). The data fit to a single exponential. C) The reaction described above was performed using varying concentrations of amicyanin. Error bars are indicated.

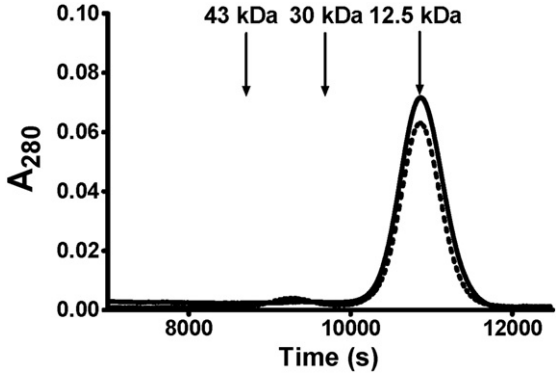

Fig. 7. Determination of the monomeric state of Co^{2+}-loaded 6×His-tagged amicyanin. Proteins were analyzed by size exclusion chromatography as described in Section 2 Materials and methods. The positions of elution of molecular weight marker proteins are indicated. The elution profiles of native amicyanin (dotted line) and Co^{2+}-loaded 6×His-tagged amicyanin (solid line) are shown.

cofactors that are metals (e.g., iron), an organic compound (e.g., flavin), or an organometallic compound (e.g., heme). Various approaches have been developed to introduce new redox centers into proteins. One approach has been de novo design of proteins that will bind redox centers such as hemes or metals [31–34]. Another approach is to covalently attach an organometallic complex to specific amino acid residues on the surface of a protein. For example, ruthenium complexes have been used extensively as a tool to study electron transfer reactions through proteins [35,36]. The use of non-protein biomimetic molecules to catalyze reactions has also been explored [37,38]. Most approaches that have been used to date require either chemical synthesis or semi-synthesis of organometallic compounds. An important requirement for the engineered redox center is a mechanism by which to initiate the reaction. This is typically achieved by photoactivation of the redox center by a laser to generate a potent oxidant or reductant that will react specifically with another redox center or substrate. The approach of incorporating Co^{2+} into a 6×His-tag to catalyze oxidation reactions was inspired by the commonly used laboratory demonstration in which $CoCl_2$ is shown to catalyze the oxidation of tartaric acid by H_2O_2 [39].

The results presented here demonstrate the utility of a relatively simple and inexpensive method for the introduction of a potent oxidizing species into a specific site on a protein for potential use as a catalyst. Plasmids are commercially available that can be used to add a 6×His-tag to either the N-terminus or C-terminus of a cloned gene. Alternatively, the 6×His-tag may be added by directed mutagenesis, not only to the ends of the proteins but possibly to other sites on the surface of the protein. This approach requires no chemical synthesis to produce or attach the cofactor, nor does it require a laser

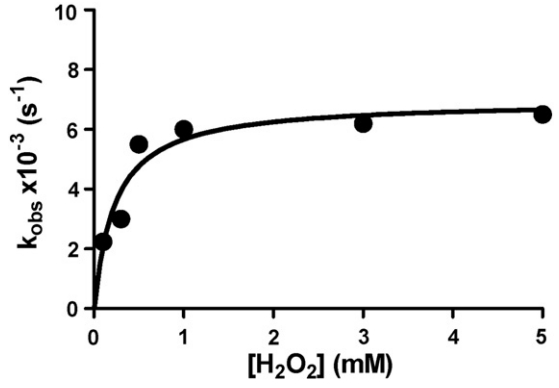

Fig. 8. Dependence of the rate of reaction of Co^{2+}-loaded 6×His-tagged amicyanin on $[H_2O_2]$. Reactions were performed as in Fig. 6 with the reactions initiated by addition of varying concentrations of H_2O_2. The line is a fit of the data by Eq. (1).

or flash system to initiate the reaction. While H_2O_2 may be considered a non-innocent and non-selective reagent, in the TTQ biosynthesis reaction it was able to drive catalysis at 100 μM concentration. Non-specific oxidation of amino acid residues at this concentration should not be a problem for most proteins. While proteins that contain redox cofactors may be more susceptible to H_2O_2 oxidation, the application of this method would not be to modify proteins that already have redox cofactors but to introduce the Co^{2+}-loaded 6×His-tag into proteins that do not have such cofactors to convert them into redox enzymes.

The preliminary characterization of the Co^{2+}-loaded 6×His-tag site has provided some intriguing insight into the nature of the site and its reaction mechanism. As the ratio of amicyanin to cobalt is 1:2, the 6×His-tag appears to form a dinuclear cobalt complex. It is conceivable that for each Co^{2+}, two N ligands are provided by different His residues within the 6×His-tag. This would allow enough space to accommodate two Co^{2+} ions. This would be comparable to the coordination that is seen when His-tagged proteins bind to the metal of the nitriloacetic acid (NTA) affinity resin during protein purification [40]. The mechanism of the Co^{2+} oxidation by H_2O_2 most likely involves a peroxo complex at the dinuclear metal site. Model complexes have been isolated of a Co^{3+}–Co^{3+} peroxo, as well as spectral evidence of a dinuclear Co^{2+}–Co^{2+} engineered protein reacting with peroxide [41–43]. In the latter case absorbance in the 300–400 nm region was observed for the cobalt-bound protein in which His residues provided the ligands [43]. These results provide a basis for future studies to characterize the metal coordination and reactivity of the Co^{2+}-loaded 6×His-tag.

These results suggest that other proteins could be engineered by introduction of a Co^{2+}-loaded 6×His-tag to catalyze the H_2O_2-dependent oxidation of a substrate that specifically binds to that protein. This approach has the potential for further refinement. The 6×His-tag could be modified to improve metal coordination or alter the redox properties of the metal. The protein to which it is attached could also be further modified by site-directed mutagenesis to improve the electron transfer efficiency for the reaction. These results provide proof of principle for this method.

Acknowledgements

This research was supported by the National Institute of General Medical Sciences of the National Institutes of Health under award number R37GM41574 (VLD).

References

[1] Y. Wang, M.E. Graichen, A. Liu, A.R. Pearson, C.M. Wilmot, V.L. Davidson, MauG, a novel diheme protein required for tryptophan tryptophylquinone biogenesis, Biochemistry 42 (2003) 7318–7325.
[2] V.L. Davidson, Pyrroloquinoline quinone (PQQ) from methanol dehydrogenase and tryptophan tryptophylquinone (TTQ) from methylamine dehydrogenase, Adv. Protein Chem. 58 (2001) 95–140.
[3] W.S. McIntire, D.E. Wemmer, A. Chistoserdov, M.E. Lidstrom, A new cofactor in a prokaryotic enzyme: tryptophan tryptophylquinone as the redox prosthetic group in methylamine dehydrogenase, Science 252 (1991) 817–824.
[4] E.T. Yukl, F. Liu, J. Krzystek, S. Shin, L.M. Jensen, V.L. Davidson, C.M. Wilmot, A. Liu, Diradical intermediate within the context of tryptophan tryptophylquinone biosynthesis, Proc. Natl. Acad. Sci. U. S. A. 110 (2013) 4569–4573.
[5] X. Li, R. Fu, S. Lee, C. Krebs, V.L. Davidson, A. Liu, A catalytic di-heme bis-Fe(IV) intermediate, alternative to an Fe(IV)═O porphyrin radical, Proc. Natl. Acad. Sci. U. S. A. 105 (2008) 8597–8600.
[6] L.M. Jensen, R. Sanishvili, V.L. Davidson, C.M. Wilmot, In crystallo posttranslational modification within a MauG/pre-methylamine dehydrogenase complex, Science 327 (2010) 1392–1394.
[7] B. Giese, M. Graber, M. Cordes, Electron transfer in peptides and proteins, Curr. Opin. Chem. Biol. 12 (2008) 755–759.
[8] J.J. Warren, M.E. Ener, A. Vlcek Jr., J.R. Winkler, H.B. Gray, Electron hopping through proteins, Coord. Chem. Rev. 256 (2012) 2478–2487.
[9] N. Abu Tarboush, L.M.R. Jensen, E.T. Yukl, J. Geng, A. Liu, C.M. Wilmot, V.L. Davidson, Mutagenesis of tryptophan199 suggests that hopping is required for MauG-dependent tryptophan tryptophylquinone biosynthesis, Proc. Natl. Acad. Sci. U. S. A. 108 (2011) 16956–16961.
[10] M. Choi, S. Shin, V.L. Davidson, Characterization of electron tunneling and hole hopping reactions between different forms of MauG and methylamine dehydrogenase within a natural protein complex, Biochemistry 51 (2012) 6942–6949.

[11] S. Shin, M. Feng, Y. Chen, L.M. Jensen, H. Tachikawa, C.M. Wilmot, A. Liu, V.L. Davidson, The tightly bound calcium of MauG is required for tryptophan tryptophylquinone cofactor biosynthesis, Biochemistry 50 (2011) 144–150.
[12] Y. Chen, S.G. Naik, J. Krzystek, S. Shin, W.H. Nelson, S. Xue, J.J. Yang, V.L. Davidson, A. Liu, Role of calcium in metalloenzymes: effects of calcium removal on the axial ligation geometry and magnetic properties of the catalytic diheme center in MauG, Biochemistry 51 (2012) 1586–1597.
[13] M. Husain, V.L. Davidson, An inducible periplasmic blue copper protein from *Paracoccus denitrificans*. Purification, properties, and physiological role, J. Biol. Chem. 260 (1985) 14626–14629.
[14] R. Durley, L. Chen, L.W. Lim, F.S. Mathews, V.L. Davidson, Crystal structure analysis of amicyanin and apoamicyanin from *Paracoccus denitrificans* at 2.0 Å and 1.8 Å resolution, Protein Sci. 2 (1993) 739–752.
[15] M. Choi, V.L. Davidson, Cupredoxins—a study of how proteins may evolve to use metals for bioenergetic processes, Metallomics 3 (2011) 140–151.
[16] C. Dennison, Investigating the structure and function of cupredoxins, Coord. Chem. Rev. 249 (2005) 3025–3054.
[17] E.I. Solomon, R.K. Szilagyi, S. DeBeer George, L. Basumallick, Electronic structures of metal sites in proteins and models: contributions to function in blue copper proteins, Chem. Rev. 104 (2004) 419–458.
[18] R.J. Van Spanning, C. Wansell, N. Harms, L.F. Oltmann, A.H. Stouthamer, Mutagenesis of the gene encoding cytochrome *c*550 of *Paracoccus denitrificans* and analysis of the resultant physiological effects, J. Bacteriol. 172 (1990) 986–996.
[19] A.R. Pearson, T. De La Mora-Rey, M.E. Graichen, Y. Wang, L.H. Jones, S. Marimanikkupam, S.A. Agger, P.A. Grimsrud, V.L. Davidson, C.M. Wilmot, Further insights into quinone cofactor biogenesis: probing the role of mauG in methylamine dehydrogenase tryptophan tryptophylquinone formation, Biochemistry 43 (2004) 5494–5502.
[20] A.Y. Chistoserdov, J. Boyd, F.S. Mathews, M.E. Lidstrom, The genetic organization of the *mau* gene cluster of the facultative autotroph *Paracoccus denitrificans*, Biochem. Biophys. Res. Commun. 184 (1992) 1181–1189.
[21] V.L. Davidson, D. Sun, Lysozyme-osmotic shock methods for localization of periplasmic redox proteins in bacteria, Methods Enzymol. 353 (2002) 121–130.
[22] M. Husain, V.L. Davidson, Purification and properties of methylamine dehydrogenase from *Paracoccus denitrificans*, J. Bacteriol. 169 (1987) 1712–1717.
[23] M. Husain, V.L. Davidson, Characterization of two inducible periplasmic *c*-type cytochromes from *Paracoccus denitrificans*, J. Biol. Chem. 261 (1986) 8577–8580.
[24] X. Li, L.H. Jones, A.R. Pearson, C.M. Wilmot, V.L. Davidson, Mechanistic possibilities in MauG-dependent tryptophan tryptophylquinone biosynthesis, Biochemistry 45 (2006) 13276–13283.
[25] V.L. Davidson, H.B. Brooks, M.E. Graichen, L.H. Jones, Y.L. Hyun, Detection of intermediates in tryptophan tryptophylquinone enzymes, Methods Enzymol. 258 (1995) 176–190.
[26] V.L. Davidson, C.M. Wilmot, Posttranslational biosynthesis of the protein-derived cofactor tryptophan tryptophylquinone, Annu. Rev. Biochem. 82 (2013) 531–550.
[27] M. Husain, V.L. Davidson, A.J. Smith, Properties of *Paracoccus denitrificans* amicyanin, Biochemistry 25 (1986) 2431–2436.
[28] R.A. Marcus, N. Sutin, Electron transfers in chemistry and biology, Biochim. Biophys. Acta 811 (1985) 265–322.
[29] I.V. Kurnikov, HARLEM Computer Program, University of Pittsburg, 2000. (http://harlem.chem.cmu.edu , in).
[30] C.C. Page, C.C. Moser, X. Chen, P.L. Dutton, Natural engineering principles of electron tunnelling in biological oxidation–reduction, Nature 402 (1999) 47–52.
[31] J. Zhuang, J.H. Amoroso, R. Kinloch, J.H. Dawson, M.J. Baldwin, B.R. Gibney, Design of a five-coordinate heme protein maquette: a spectroscopic model of deoxymyoglobin, Inorg. Chem. 43 (2004) 8218–8220.
[32] Y. Lu, N. Yeung, N. Sieracki, N.M. Marshall, Design of functional metalloproteins, Nature 460 (2009) 855–862.
[33] B.M. Discher, R.L. Koder, C.C. Moser, P.L. Dutton, Hydrophilic to amphiphilic design in redox protein maquettes, Curr. Opin. Chem. Biol. 7 (2003) 741–748.
[34] V. Nanda, M.M. Rosenblatt, A. Osyczka, H. Kono, Z. Getahun, P.L. Dutton, J.G. Saven, W.F. DeGrado, De novo design of a redox-active minimal rubredoxin mimic, J. Am. Chem. Soc. 127 (2005) 5804–5805.
[35] B. Durham, F. Millett, Design of photoactive ruthenium complexes to study electron transfer and proton pumping in cytochrome oxidase, Biochim. Biophys. Acta 1817 (2012) 567–574.
[36] J.N. Onuchic, D.N. Beratan, J.R. Winkler, H.B. Gray, Pathway analysis of protein electron-transfer reactions, Annu. Rev. Biophys. Biomol. Struct. 21 (1992) 349–377.
[37] M. Costas, K. Chen, L. Que Jr., Biomimetic nonheme iron catalysts for alkane hydroxylation, Coord. Chem. Rev. 200–202 (2000) 517–544.
[38] H. Maid, P. Böhm, S.M. Huber, W. Bauer, W. Hummel, N. Jux, H. Gröger, Iron catalysis for in situ regeneration of oxidized cofactors by activation and reduction of molecular oxygen: a synthetic metalloporphyrin as a biomimetic NAD(P)H oxidase, Angew. Chem. Int. Ed. 50 (2011) 2397–2400.
[39] P.T. Ruda, Versatile kinetics demonstration, J. Chem. Educ. 55 (1978) 652.
[40] S.V. Wegner, J.P. Spatz, Cobalt(III) as a stable and inert mediator ion between NTA and His6-tagged proteins, Angew. Chem. Int. Ed. Engl. 52 (2013) 7593–7596.
[41] N. Kitajima, S. Hikichi, M. Tanaka, Y. Morooka, Fixation of atmospheric Co2 by a series of hydroxo complexes of divalent metal-ions and the implication for the catalytic role of metal-ion in carbonic-anhydrase — synthesis, characterization, and molecular-structure of [Lm(Oh)]N (N = 1 or 2) and Lm(Mu-Co3)Ml (M(Ii) = Mn, Fe, Co, Ni, Cu, Zn L = Hb(3,5-Ipr2pz)3), J. Am. Chem. Soc. 115 (1993) 5496–5508.
[42] S. Hikichi, H. Komatsuzaki, N. Kitajima, M. Akita, M. Mukai, T. Kitagawa, Y. Morooka, Characterization of a mu-eta(2):eta(2)-peroxo dinuclear cobalt(II) complex, Inorg. Chem. 36 (1997) 266–267.
[43] D.E. Benson, A.E. Haddy, H.W. Hellinga, Converting a maltose receptor into a nascent binuclear copper oxygenase by computational design, Biochemistry 41 (2002) 3262–3269.